Quasi-free photoproduction of η-mesons off the neutron

I. Jaegle[1], T. Mertens[1], A.V. Anisovich[2,3], J. C. S. Bacelar[4], B. Bantes[5], O. Bartholomy[2], D. Bayadilov[2,3], R. Beck[2], Y.A. Beloglazov[3], R. Castelijns[4], V. Crede[2,6], H. Dutz[5], A. Ehmanns[2], D. Elsner[5], K. Essig[2], R. Ewald[5], I. Fabry[2], M. Fuchs[2], Ch. Funke[2], R. Gothe[5], R. Gregor[7], A. B. Gridnev[3], E. Gutz[2], S. Höffgen[5], P. Hoffmeister[2], I. Horn[2], J. Junkersfeld[2], H. Kalinowsky[2], S. Kammer[5] V. Kleber[5] Frank Klein[5], Friedrich Klein[5], E. Klempt[2], M. Konrad[5], M. Kotulla[1,7], B. Krusche[1], M. Lang[2], J. Langheinrich[5], H. Löhner[4], I.V. Lopatin[3], J. Lotz [2], S. Lugert[7], D. Menze[5], J.G. Messchendorp[4], V. Metag[7], C. Morales[5], M. Nanova[7], V.A. Nikonov[2,3], D. Novinski[2,3], R. Novotny[7], M. Ostrick[5], L.M. Pant[7], H. van Pee[2,7], M. Pfeiffer [7], A. Radkov[3], A. Roy[8], A.V. Sarantsev[2,3], S. Schadmand[7], C. Schmidt[2], H. Schmieden[5], B. Schoch[5], S. Shende[4], V. Sokhoyan[2], A. Süle[5], V.V. Sumachev[3], T. Szczepanek[2], U. Thoma[2,7], D. Trnka[7], R. Varma[7], D. Walther[5], Ch. Weinheimer[2], Ch. Wendel[2]
(The CBELSA/TAPS Collaboration)
[1] *Department Physik, Universität Basel, Switzerland*
[2] *Helmholtz-Institut für Strahlen- u. Kernphysik, Universität Bonn, Germany*
[3] *Petersburg Nuclear Physics Institute, Gatchina, Russia*
[4] *KVI, Groningen, The Netherlands*
[5] *Physikalisches Institut, Universität Bonn, Germany*
[6] *Department of Physics, Florida State University, Tallahassee, USA*
[7] *II. Physikalisches Institut, Universität Gießen, Germany*

(Dated: January 5, 2008)

Quasi-free photoproduction of η-mesons off nucleons bound in the deuteron has been measured with the CBELSA/TAPS detector at the Bonn ELSA accelerator for incident photon energies up to 2.5 GeV. The η-mesons have been detected in coincidence with recoil protons and recoil neutrons, which allows a detailed comparison of the quasi-free $n(\gamma,\eta)n$ and $p(\gamma,\eta)p$ reactions. The excitation function for η-production off the neutron shows a pronounced bump-like structure at incident photon energies around 1 GeV and a smaller one around 1.8 GeV, which are absent for the proton, indicating different contributions of nucleon resonances. The invariant mass distribution of η-mesons and recoil neutrons shows also a narrow structure with a width comparable to the instrumental resolution.

PACS numbers: PACS numbers: 13.60.Le, 14.20.Gk, 14.40.Aq, 25.20.Lj

The excitation spectrum of the nucleon is closely connected to the properties of Quantum-Chromo Dynamics (QCD) in the low-energy regime, where it cannot be treated in perturbative approaches. Lattice gauge calculations have provided results for the ground state properties, and more recently also for some excited states (see e.g. Ref. [1]), but the prediction of the full excitation spectrum is still out of reach. The connection between experimental observations and QCD is mostly done with QCD inspired quark models. However, so far a comparison of the known excitation spectrum to model predictions reveals severe problems for all models. The ordering of some of the lowest lying states like the $N(1440)P_{11}$ ('Roper') and the first excited Δ, the $P_{33}(1600)$, is in general not reproduced. Furthermore, all models predict many more states than have been observed. Most states have been observed with elastic scattering of charged pions. It is thus possible that the data base is biased towards states that couple strongly to πN. Therefore photon induced reactions, which nowadays can be investigated with comparable precision as hadron induced reactions, have moved into the focus.

Experiments for the study of the free proton are well developed, but much less effort has gone into the investigation of the excitation spectrum of the neutron, which is complicated by the non-availability of free neutrons. However, such measurements are required for the extraction of the isospin structure of the electromagnetic excitations. An excellent example is photo- and electroproduction of η mesons. This reaction has been studied in detail off the free proton [2–12], where in the threshold region it is dominated by the excitation of the $S_{11}(1535)$ resonance [13]. Photon beam asymmetries [3, 11] and angular distributions [2, 9, 10] reveal a small contributions from the $D_{13}(1520)$ resonance via an interference with the S_{11}. Further weak contributions of higher lying resonances have been suggested by detailed analyses of the data with different models (see e.g. [14, 15]).

The investigation of η photoproduction off ^{2}H and ^{3,4}He [16–22] has clarified the isospin structure of the $S_{11}(1535)$ electromagnetic excitation, which is dominantly iso-vector [23] with a value of 2/3 for the neutron/proton cross section ratio. At energies above the $S_{11}(1535)$, models predict a rise of the ratio due to higher lying resonances. In the work of Chiang et al. [14] ('Eta-MAID'), the largest contribution comes from the $D_{15}(1675)$, which has a strong electromagnetic coupling to the neutron [24]. However, also in the framework of the chiral soliton model [25] such a state is predicted. This is the nucleon-like (P_{11}) member of the predicted anti-decuplet of pentaquarks. Very recently, Kuznetsov et al. [26] reported a structure in the excitation function

of η production off quasi-free neutrons, which they interpreted as tentative evidence for a narrow resonance ($\Gamma <$ 30 MeV) at an excitation energy around 1.68 GeV.

Here we report a measurement of angular distributions and total cross sections for quasi-free photoproduction of η mesons off protons and neutrons bound in the deuteron for incident photon energies up to 2.5 GeV. The experiment was done at the tagged photon facility of the Bonn ELSA accelerator [27, 28] with the combined Crystal Barrel [29] and TAPS [30, 31] calorimeters. The setup is described in [11]. The liquid deuterium target of 5.3 cm length was mounted in the center of the Crystal Barrel and surrounded by a three-layer scintillating fiber detector [32] for charged particle identification.

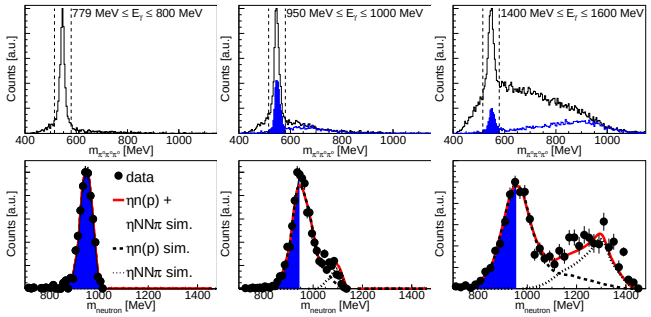

FIG. 1: Upper row: three-π^o invariant mass. Filled histograms: after cut on missing mass. Bottom row: missing mass spectra after cut on invariant mass and subtraction of background. Curves: Monte Carlo simulations of $\gamma d \to np\eta$ and $\gamma d \to np\eta\pi$. Colored part of peaks: accepted events. All data in coincidence with neutrons.

Photoproduction of η mesons was studied via the $\eta \to 3\pi^o \to 6\gamma$ decay (the two-photon decay was not used due to trigger restrictions). Events with at least six neutral hits were accepted if they could be combined to three π^o mesons (invariant mass cut: 110 MeV $< m_{\gamma,\gamma} <$ 160 MeV). For further analysis, these events were grouped into the following (partly overlapping) sub-sets: events with any number of further hits (totel inclusive including $\eta\pi$ final states), events with none or one further hit (total quasi-free η off deuteron), events with six neutral hits and one charged hit (quasi-free proton cross section), and events with exactly seven neutral hits (quasi-free neutron cross section). Typical spectra of the three-π^o invariant mass of events in coincidence with a recoil neutron are shown in fig. 1. In this part of the analysis, recoil nucleons were treated as missing particles. Their missing mass (bottom part of fig. 1) was calculated under the assumption of quasi-free meson production on a nucleon at rest. The Fermi motion of the bound nucleons broadens the peaks, however it was still possible to separate single η production from the $\eta\pi$ final state. A very conservative missing mass cut was used, in order to avoid any contamination from $\eta\pi$.

Recoil protons and neutrons in TAPS were identified with the plastic veto detectors in front of the BaF_2 crystals and a time-of-flight versus energy analysis. Protons in the barrel were accepted when at least two out of the three layers of the Inner-detector had responded within an angular difference of 10^o to a hit in the barrel. Barrel hits were accepted as 'neutral' when no layer of the Inner-detector had responded. A direct separation of neutrons and photons in the barrel was not possible. In events with seven neutral hits first six hits were assigned by the invariant mass analysis to the $\eta \to 3\pi^o \to 6\gamma$ decay-chain and the left-over hit was taken as neutron.

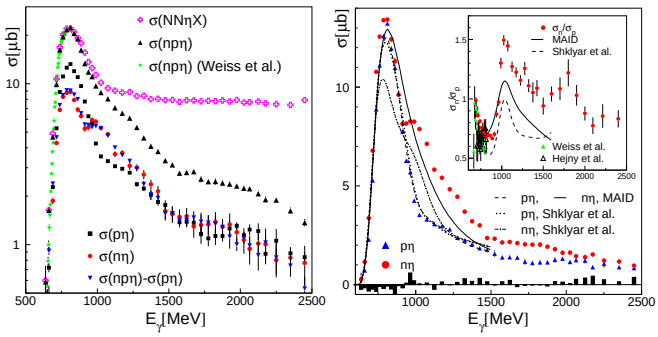

FIG. 2: Left hand side: Total cross sections for all final states (see text). Previous data for σ_n/σ_p from ref. [18, 21]. Right hand side: quasi-free cross sections off proton and neutron . Bar charts: $(\sigma_n - (\sigma_{np} - \sigma_p))/2$. Curves: model predictions (MAID model [14]), Shklyar et al. [36]) all folded with Fermi motion. Neutron data and curves scaled up by factor of 3/2.

Absolute cross sections were derived from the target density (surface number density 0.26 b^{-1}), the incident photon flux, the decay branching ratio (31.35 %), the detection efficiency of the $\eta \to 6\gamma$ decay, and the detection efficiency for neutrons and protons. The photon flux was determined by counting the deflected electrons and measuring the tagging efficiency (i.e. the fraction of correlated photons which pass the collimator) with a detector placed directly in the photon beam. Data have been taken in two runs with different photon fluxes (2.6 and 3.2 GeV electron energy, linearly polarized and unpolarized photons). The results agree within ±10 %. They have been averaged and the systematic uncertainty of the flux is estimated as 10 %. The detection efficiency for the η decay was determined with Monte Carlo simulations (GEANT3 package [33]) as discussed in Ref. [34] for pion production. For neutrons and protons the detection efficiency was also simulated (typical values: 30 % for neutrons, 90 % for protons), and for protons additionally determined from the analysis of η production off the free proton (agreement between simulation and data better than 10 %). Total systematic uncertainties (including efficiencies, cuts, and the fit of the small residual background in the invariant mass spectra, but not the flux) have been estimated as 10 % below incident photon energies of 1.5 GeV, 15 % between 1.5 - 2 GeV, and below 20 % above 2 GeV for the reaction with coincident neutrons. They are below 10 % for the proton channel be-

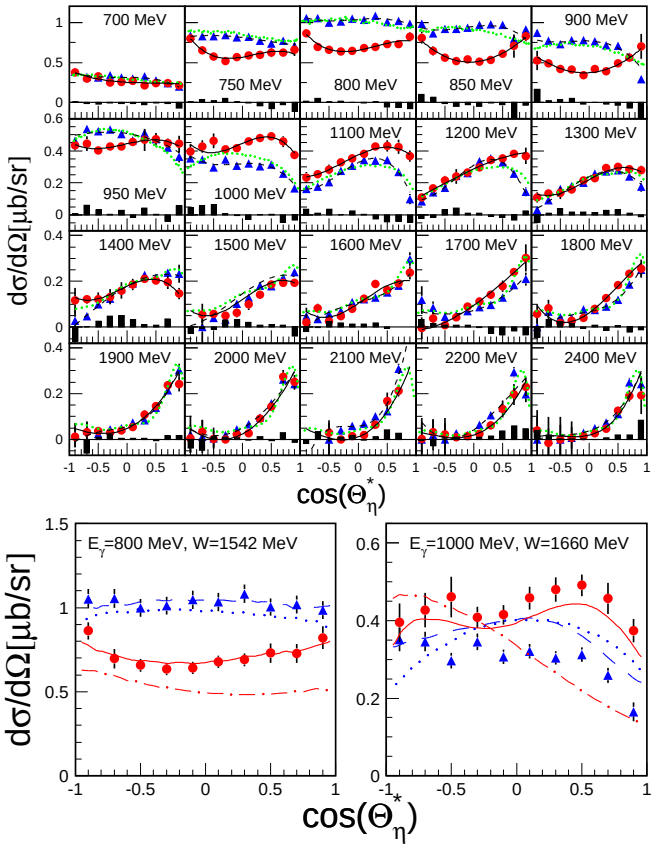

FIG. 3: Angular distributions: (Blue) triangles: quasi-free proton, (red) circles: quasi-free neutron. Upper part: (black) dashed and solid lines: fit of proton and neutron data (see text), bar charts: half difference of σ_n and $\sigma_{np} - \sigma_p$. (Green) dotted curves: free proton results [9] folded with Fermi motion. Bottom part: Angular distributions at 0.8 and 1.0 GeV and model predictions (Fermi folded), solid: MAID n, dashed MAID p [14]; dotted p, dash-dotted n Ref. [36].

low 2 GeV and 15 % above. The only uncertainty, which does not cancel in the neutron/proton ratio, comes from the detection of the recoil nucleons. The data were analyzed for η mesons in coincidence with recoil protons (σ_p), with recoil neutrons (σ_n), and without any condition for recoil nucleons (σ_{np}) including also the events without detected nucleons. Since coherent production can be neglected, we expect $\sigma_{np} = \sigma_p + \sigma_n$. Consequently, the neutron cross section can be determined in two independent ways, based on neutron detection (σ_n) or on proton detection ($\sigma_{np} - \sigma_p$). The results are in good agreement (see figs. 2,3) and the differences are an independent estimate for the systematic uncertainties.

The total cross sections, which have been obtained by integration of the angular distributions, are summarized in fig. 2. The inclusive cross section for the ηNNX final state (no conditions for recoil nucleons, no missing mass cut) agrees with the ηnp cross section (no condition on recoil nucleon, but cut on missing mass) below the $\eta\pi$ production threshold (≈800 MeV). At higher energies,

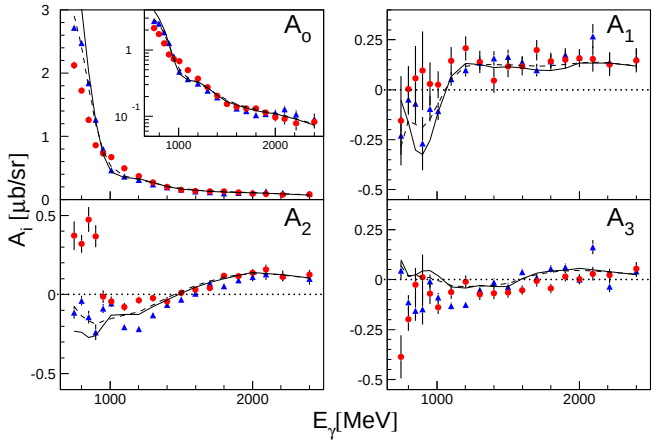

FIG. 4: Legendre coefficients of angular distributions. Circles: quasi-free neutron, triangles quasi-free proton, solid line: free proton, dashed line: free proton Fermi smeared.

contributions from $\eta\pi$ become dominant. The result for ηnp below 800 MeV agrees with a previous measurement with TAPS at MAMI [21].

The two data sets for the neutron cross section are in excellent agreement and show a bump-like structure around 1 GeV. They have been averaged and are compared to the proton data and to model calculations [14, 36] in the right hand side of fig. 2. The model results have been folded with the momentum distribution of the bound nucleons [35] as discussed in [16]. Both models show a peak-like structure in the cross section ratio around 1 GeV, although less pronounced as in the data. However, the mechanisms (strong contribution of $D_{15}(1675)$ resonance [14] versus S_{11}, P_{11} coupled-channel effects [36]) are quite different.

Differential cross sections in the cm system of the incident photon and a nucleon at rest (see [16] for details) are shown in fig. 3. The results for the quasi-free proton are in agreement with the free proton distributions folded with Fermi motion. The distributions have been fitted with Legendre polynomials $P_i(cos(\Theta^\star_\eta))$, related to the contributing partial waves [23]:

$$\frac{d\sigma}{d\Omega} = \frac{q^\star_\eta}{k^\star_\gamma} \sum_i A_i P_i(cos(\Theta^\star_\eta)) \qquad (1)$$

where the A_i are expansion coefficients. The phase-space factor $q^\star_\eta/k^\star_\gamma$ is also evaluated for the above cm system. The results for $A_0, ..., A_4$ are shown in fig. 4. In the region of the dominant $S_{11}(1535)$, the s-wave contributions (A_0) reflect the ratio of the helicity couplings of this resonance [23], and the shape of the angular distributions reflects the interference with the $D_{13}(1520)$ (see ref. [21]). In an approximation taking into account only contributions from these two resonances [21], the A_2 coefficient is directly proportional to the product of their helicity-1/2 couplings. This implies a positive sign for A_2^n, a negative sign for A_2^p, and a larger absolut value

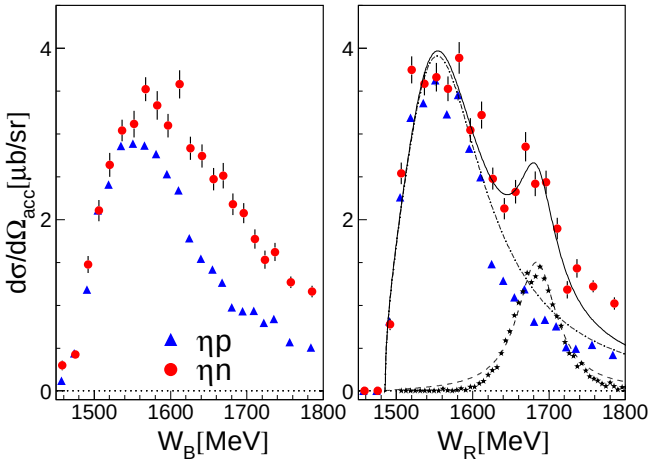

FIG. 5: Proton and neutron excitation functions for $cos(\Theta^{\star}_{\eta}) < -0.1$ without and with event-by-event correction of Fermi motion. Curves: solid: full fit, dash-dotted: BW-curve of $S_{11}(1535)$, dashed: BW-curve for second structure. Stars: response for a δ-function due to finite energy resolution.

of A_2^n, all in agreement with the data. In this energy region, the angular distributions for proton and neutron are well described by the MAID model [14] (see fig. 3). The angular distributions for protons and neutrons are similar for high incident photon energies, where diffractive t-channel processes make a large contribution [9, 10]. In the most interesting region around 1 GeV, the shape of the angular distributions for the neutron changes rapidly, however, apart from A_o the Legendre coefficents for proton and neutron are similar. In this region, the neutron data (see fig. 3) is reasonably well reproduced by the MAID model [14] with a large $N\eta$-decay branching ratio (17 %) of the $D_{15}(1675)$ (PDG quotes 0±1 %). Recently, Shklyar, Lenske, and Mosel [36] have presented results from a coupled-channel effective Lagrangian approach, where they try to explain the data with coupled channel effects involving $S_{11}(1535)$, $S_{11}(1650)$, and $P_{11}(1710)$. The shape of their angular distributions is not in good agreement with the data (see fig. 3, right hand side). A partial wave analysis in the framework of the Bonn-Gatchina model [15], which will be published elsewhere, can also reproduce the bump-structure and the angular distributions alternatively with either interference effects in the S_{11} sector, or with an additional P_{11} state. Consequently, so far no definitive conclusion can be drawn about the structure around 1 GeV.

Due to the Fermi smearing, it is difficult to discriminate between scenarios with very narrow states and broader resonances. Fix, Tiator, and Polyakov [37] find comparable results for the MAID model with strong D_{15} contribution and for a model with a P_{11} as narrow as 10 - 30 MeV. In principle, Fermi motion can be corrected event-by-event when energy and momentum of the recoil nucleons are known. Instead of using the total cm energy W_B deduced from the incident photon energy, it can be reconstructed from the four-vectors of the η meson and the recoil nucleon (W_R). Since the energy of the neutrons is measured by time-of-flight, only neutrons in TAPS, which correspond to η mesons with $\cos(\Theta^{\star}_{\eta}) < -0.1$ can be used. The results are summarized in fig. 5. For proton and neutron, the correction leads to the expected narrower peak for the $S_{11}(1535)$. However, for the neutron also a narrow structure around 1 GeV appears. The neutron data was fitted with the sum of two Breit-Wigner (BW) curves corresponding to the $S_{11}(1535)$ [13] and the structure around 1 GeV. The parameters for the S_{11} (position: 1566 MeV, width: 162 MeV) are similar to a fit of the free proton data (1540 MeV, 162 MeV). Position and width of the second structure are 1683 MeV and (60±20) MeV. However, this width is only an upper limit, since the structure is broadened by the time-of-flight resolution. Even the simulation of a δ-function at the peak position reproduces the observed line-shape (see fig. 5), so that no lower limit of the width can be deduced.

Acknowledgments

We wish to acknowledge the outstanding support of the accelerator group and operators of ELSA. This work was supported by Schweizerischer Nationalfonds and Deutsche Forschungsgemeinschaft (SFB/TR-16.)

[1] T. Burch *et al.*, Phys. Rev. **D74** 014504 (2006).
[2] B. Krusche *et al.*, Phys. Rev. Lett. **74** 3736 (1995).
[3] J. Ajaka *et al.*, Phys. Rev. Lett. **81** 1797 (1998).
[4] A. Bock *et al.*, Phys. Rev. Lett. **81** 534 (1998).
[5] C.S. Armstrong *et al.*, Phys. Rev. **D60** 052004 (1999).
[6] R. Thompson *et al.*, Phys. Rev. Lett. **86** 1702 (2001).
[7] F. Renard *et al.*, Phys. Lett. 215 **B528** (2002).
[8] M. Dugger *et al.*, Phys. Rev. Lett. **89** 222002 (2002).
[9] V. Crede *et al.*, Phys. Rev. Lett. **94** 012004 (2005).
[10] O. Bartholomy *et al.*, Eur. Phys. J **A33** 133 (2007).
[11] D. Elsner *et al.*, Eur. Phys. J. **A33** 147 (2007).
[12] H. Denizli *et al.*, Phys. Rev. **C76** 015204 (2007).
[13] B. Krusche *et al.*, Phys. Lett. **B397** 171 (1997).
[14] W.-T. Chiang *et al.*, Nucl. Phys. **A700** 429(2002).
[15] A.V. Anisovich *et al.*, Eur. Phys. J. **A25** 427 (2005).
[16] B. Krusche *at al.*, Phys. Lett. **B358** 40 (1995).
[17] P. Hoffmann-Rothe *et al.*, Phys. Rev. Lett. **78** 4697 (1997).
[18] V. Hejny *et al.*, Eur. Phys. J. **A6** 83 (1999).
[19] J. Weiß *et al.*, Eur. Phys. J. **A11** 371 (2001).
[20] V. Hejny *et al.*, Eur. Phys. J. **A13** 493 (2002).
[21] J. Weiß *et al.*, Eur. Phys. J. **A16** 275 (2003).
[22] M. Pfeiffer *et al.*, Phys. Rev. Lett. **92** 252001 (2004).
[23] B. Krusche and S. Schadmand, Prog. Part. Nucl. Phys.

51 399 (2003).
[24] W.-M. Yao *et al.*, J. Phys., **G33** 1 (2006).
[25] R.A. Arndt *et al.*, Phys Rev. **C69** 035208 (2004).
[26] V. Kuznetsov *et al.*, Phys. Lett. **B647** 23 (2007).
[27] D. Husman, W.J. Schwille, Phys. BL. **44** 40 (1988).
[28] W. Hillert, Eur. Phys. J.**A28** 139 (2006).
[29] E. Aker *et al.*, Nucl. Instr. and Meth. **A321** 69 (1992).
[30] R. Novotny, IEEE Trans. on Nucl. Science **38**, 379 (1991).
[31] A.R. Gabler *et al.*, Nucl. Instr. and Meth. **A346** 168 (1994).
[32] G. Suft *et al.*, Nucl. INst. Meth. **A538** 416 (2005).
[33] R. Brun *et al.*, GEANT, Cern/DD/ee/84-1, (1986).
[34] B. Krusche *et al.*, Eur. Phys. J. **A22** 277 (2004).
[35] M. Lacombe *et al.*, Phys. Lett. **B101** 139 (1981).
[36] V. Shklyar *et al.*, Phys. Lett. **B650** 172 (2007).
[37] A. Fix *et al.*, Eur. Phys. J. **A32** 311 (2007)